

Coaxial Traps for HF Antennas

1. Purpose

Document impedance tests on a sample coaxial trap resonator produced by Owen Duffy, VK1OD, with a resonant frequency of approximately 6.3 MHz. Documentation includes occasional explanatory items that are tutorial in nature, since some readers may not be familiar with all aspects of Q-meter techniques.

2. Description

Inductance coil of 10 turns of coaxial cable, close wound over a length of 52 mm., on a tubular former of outside diameter 48.3 mm., length 75 mm., wall thickness 2.6 mm. Former appears to be off-white hard PVC, possibly plumbing grade, UV stabilised. Turns held in place by a covering of 2 layers of black PVC electrical tape.

Cable appears to be RG58 C/U or similar : centre conductor 19 strands of tinned copper, solid polyethylene dielectric, single tinned copper braid shield of good coverage, black PVC jacket. Length of cable estimated at 1.67 metres, plus tails at each end of 55 mm.

Normally intended connections : centre conductor at end A_f connected to braid at opposite end (A_f to B_s): antenna wires connected to uncommitted centre conductor, A_s and braid tail B_f . See figure 1 for layout.

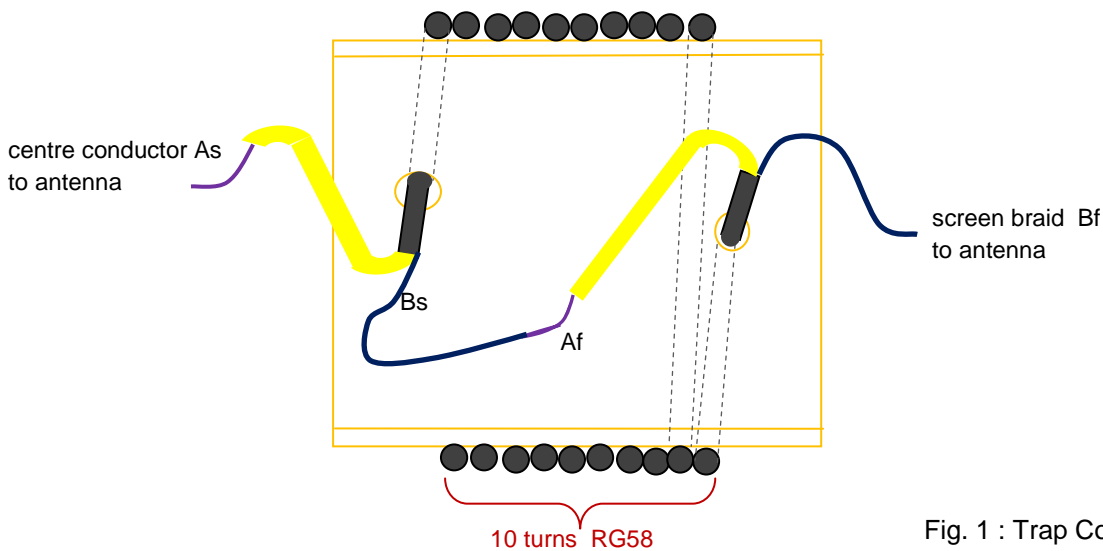


Fig. 1 : Trap Connections

3. Low Frequency Measurements

Parameter \ Instrument	Cintel Bridge @ $\omega = 10,000$ rad/sec	W-K B221 + Q221 @ $\omega = 10kr/s$
Screen Inductance $B_s - B_f$	$3.56 \mu H + 0.026 \Omega$	$3.57 \mu H + 0.032 \Omega$
Inner Inductance $A_s - A_f$	$4.30 \mu H + 0.085 \Omega$	$4.25 \mu H + 0.089 \Omega$
Series Aiding $A_s - B_f$, link $B_s - A_f$	$14.8 \mu H + 0.11 \Omega$	$14.8 \mu H + 0.123 \Omega$
Mutual $A_s - A_f$ to $B_s - B_f$	$3.50 \mu H$	$3.50 \mu H$
Coax. Loop L : $A_s - B_s$, short $A_f - B_f$	$0.59 \mu H + 0.12 \Omega$	$0.66 \mu H + 0.122 \Omega$
Coax. Capacitance $A_s - B_s$	170 pF (Marconi Brdg. @ 1 kHz)	$170.2 \text{ pF} // 0.001 \mu S$

Table 1 : Low Frequency Parameter Measurements

Measured capacitance of the coaxial cable between centre and screen is consistent with 50Ω cable, which normally measures 101 pF per metre for solid polyethylene dielectric. Measured inductance of the coaxial cable with a short circuit between A_f and B_f is high, probably due to the large parasitic inductance introduced by the cable tails at both

ends. From the geometry of the tails an additional 0.12 – 0.15 μH could have been added to the inductance of the basic coaxial cable. Note also that high frequency inductance is lower than the measured inductance value at low audio frequencies due to skin effect. At RF, 50 Ω cable usually measures ≈ 252.5 nH/metre.

4. High Frequency Measurement Technique

Most high frequency measurements at, or close to trap resonance frequency were effected using a Q-meter¹. Impedance levels at resonance are well suited to Q-meter techniques. Supplementary readings were later taken at frequencies away from resonance using RF bridge techniques where the lowered impedance level came within range of available instruments.

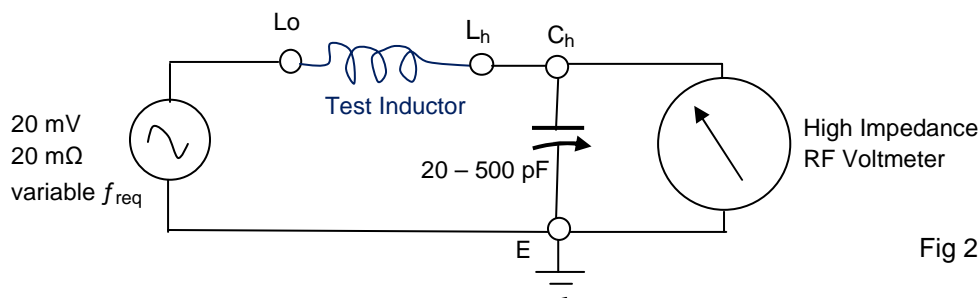


Fig 2 : Q-Meter Basic Layout

With the variable capacitor adjusted for resonance at the test frequency, the ratio of the voltmeter reading to the excitation voltage ≈ inductor Q-factor : variable air capacitor Q ≈ 30,000 at the frequencies involved and source resistance is small so these loss factors can usually be ignored. A frequency counter was used for measurement of source frequency to improve accuracy over that afforded by the oscillator frequency dial.

To estimate test inductor stray winding capacitance, C₀, including the *effective value* of any added capacitance across inductor turns, a frequency doubling method can be used. First resonate the inductor at frequency f₁ with a large value for the variable capacitor = C₁. Then increase the test frequency to 2×f₁ and readjust the capacitor for resonance = C₂.

$$C_0 = \frac{C_1 - 4C_2}{3}$$

5. Results for Full Trap

With A_s to L_h and B_f to L_o, i.e. the bootstrap connection, measured values were :-

Frequency MHz	2.5	3.0	3.5	4.0	5.0	6.33 *	6.36 *
Capacitance Dial pF	238	151	99	65	26	no change	no change
Q _{ind} = reading on meter	81	78	73	65	44	127 *	115 *
Dial Capacitance to resonate with L _{aux} = 4.8 μH alone						128 pF *	125 pF *
Q _a . for L _{aux} only	(Q _{ind} = value when L of trap under test added)					185 *	180*
Q – true : trap (corrected for C ₀)	96	101	105	109	118	139	112
Impedance @ test freq.	3.3+ j270	4.5+ j350	6.3+ j460	9.4+ j610	28+ j1k2	80k + j0	64k + j0
C ₀ effective (pF)	44.7 pF (2.5/5 MHz)					43.5	

Table 2: Q- measured results for Full Trap with centre and screen in series aiding.

Frequency doubling provides an initial estimate of 44.7 pF for the *effective value* of the cable capacitance plus stray winding capacitance, as seen by the series aiding connection of the centre and screen conductors. Estimated effective

¹ Also known as a "Circuit Magnification Meter" from the voltage stepup that occurs between source and detector.

A restored Marconi TF1245 circa 1959 was used for the tests : Reasonable trap Q-factors, typically > 10 are required.

inductance is 14.3 μH , so the trap should display a parallel resonance ≈ 6.29 MHz. Measurement with a dip oscillator and frequency counter confirmed existence of a sharp parallel resonance at 6.33 MHz.

* Measurements were refined by the 'natural resonance' method using an auxiliary inductor² of 4.8 μH . Connected between Lo and Lh, the 4.8 μH inductor resonated at 6.33 MHz with $C_{\text{dial}}=128$ pF, $Q_a = 185$. When the trap was connected in parallel across Lo-Lh the resonant frequency remained unaltered but the indicated Q-value dropped to 127. So the resonant trap was appearing as a pure resistance³ at this frequency. Denoting this natural resonance frequency as f_0 , frequency and capacitance at 2.5 MHz as f_1 and C_1 , capacitance resonating auxiliary inductor as C_2 , Q of the auxiliary inductor alone as Q_a , and Q for auxiliary in parallel with the trap as Q_{+t} :

$$C_0 = \frac{C_1}{(f_0 / f_1)^2 - 1} \quad L = \frac{1}{\omega_0^2 \cdot C_0} \quad R_{xp} = \frac{Q_a \cdot Q_{+t}}{Q_a - Q_{+t}} \cdot \frac{1}{\omega_0 \cdot C_2}$$

R_{xp} is the parallel resistance of the trap at resonance. $L = 14.4$ μH is the effective inductance of the trap at resonance. In the presence of stray winding capacitance and/or added capacitance across the inductor, C_0 , the indicated Q-value is lower than the true Q-value of the resonant circuit. Correction to obtain Q_{true} is :-

$$Q_{\text{true}} = Q_{\text{indicated}} \left(1 + \frac{C_0}{C_{\text{dial}}} \right)$$

$$\text{Trap impedance @ test frequency } Z_t = \frac{1}{Q_{\text{ind}} \cdot \omega \cdot C_{\text{dial}}} + j \frac{1}{\omega \cdot C_{\text{dial}}}$$

Trap impedance at resonance was found to be highly sensitive to test conditions, including proximity to such objects as metal panels or lossy dielectrics, including test personnel. Tabulated values are pessimistic worst cases : values in the region 70 - 80k Ω were initially measured with the trap well isolated using lengthened leads. From extrapolation of the trend of Q_{true} vs. frequency, at trap resonance $Q_{\text{true}} \approx 130$, giving an estimated impedance of 74k Ω . It is possible that the latter value could be achieved when installed in isolation on an antenna, provided that moisture ingress to the windings, including between the braid and dielectric, can be prevented.

Trap observed resonant frequency fluctuated slightly, typically $< \pm 30$ kHz, depending on test conditions. This was initially attributed to parasitic capacitance changes associated with the test configuration. However it was later observed that trap frequency and Q were temperature dependent, as well as being subject to ageing and handling effects. The second set of measurements at 6.36 MHz were taken 4 weeks later than the first set.

6. Half-Trap Measurements

Q-meter measurements were made on the various possible half-trap configurations. These use either the coaxial centre conductor only as the inductive element or the braid alone as the inductive element. Capacitance between the centre conductor and the braid provides the resonating capacitance. Measurement techniques were the same as those described for the full or 'bootstrap' trap.

Two sets of readings were taken for each configuration to examine the effects of stray capacitance to ground when a normally floating component is connected in the 'earthy' Q-meter environment. Table 3 documents the results.

Slightly higher resonant impedance occurs when the centre conductor is used as the inductive element, a consequence of the marginally higher effective value of inductance and lower effective capacitance. This configuration is significantly more sensitive to stray capacitance to ground.

² Requires a physically small and well shielded inductor with a high Q-value

³ Change of resonant frequency can be detected by the requirement to either change test frequency slightly or change capacitance to restore resonance: a capacitance change of 0.2 pF was readily detectable and measurable on the Q-meter.

Q-factors at resonance were similar for all configurations, with stray parasitic capacitance having little influence on the measured Q-factor.

Connections →	As→Lh, AfBs→Lo	AfBs→Lh, As→Lo	AfBs→Lh, Bf→Lo	Bf→Lh, AfBs→Lo
3.0 MHz C_{dial} , Q_{rdg}	543 pF $Q = 58$	530 pF $Q = 59$	624 pF $Q = 76$	623 pF $Q = 82$
6.0 MHz C_{dial} , Q_{rdg}	20 pF $Q = 11$	11 pF $Q = 12$	19 pF $Q = 13$	18 pF $Q = 10$
L_{aux} 4.8 μ H C_{dial} , Q_{rdg}	125 pF $Q = 190$	133 pF $Q = 180$	130 pF $Q = 180$	130 pF $Q = 180$
ω_o MHz	6.38 MHz	6.20 MHz	6.29 MHz	6.28 MHz
L_{aux} +Trap Q_{rdg}	$Q = 60$	$Q = 60$	$Q = 52$	$Q = 52$
C_o freq. doubling	154 pF	162 pF	183 pF	184 pF
C_o by ω_o method	154 pF	162 pF	184 pF	184 pF
$L_{effective}$	4.04 μ H	3.94 μ H	3.48 μ H	3.49 μ H
R_{xp} = Resistance @ ω_o	17.5 k Ω	17.0 k Ω	14.2 k Ω	14.3 k Ω
Q_o @ ω_o resonance	$Q_o = 108$	$Q_o = 107$	$Q_o = 103$	$Q_o = 104$

Table 3 : Half-Trap Measured Characteristics

7. Impedance of Braid Inductor only at RF

Table 4 records the measured impedance of the inductor formed by the outer coaxial braid alone vs. frequency.

Frequency	5.0	6.0	7.0	10.0	12.0	40.065
C_{dial}	290 pF	199 pF	144 pF	68 pF	45pF	no change
$Q_{indicated}$	135	147	150	160	160	$\delta Q = -39$
$L_{aux} = 0.2\mu$ H : dial capacitance to resonate and Q with L_{aux} only : $\delta Q =$ change when test L added						66pF $Q=220$
Q_{true}	138	152	156	174	180	72
Z_{eff} @ freq. ⁴	0.81 + j 110	0.90 + j 133	1.05 + j 158	1.46 + j 234	1.84 + j 295	62 k Ω + j 0

Table 4 : Inductance of Outer Braid only : measure between Bs and Bf : all other leads open

Calculated $C_o = 6.3$ pF based on 6 – 12 MHz frequency doubling. Calculated Inductance $L = 3.42$ μ H.

Using the "natural frequency" method at 40.06MHz, auxiliary inductor of 0.2 μ H,

$$C_o = 4.6 \text{ pF}, \quad L = 3.44 \text{ } \mu\text{H}, \quad R_{xp} = 62 \text{ k}\Omega$$

Measured resonance with a dip meter was 49.66 MHz with the trap on the test bench and 53.06 MHz with the trap well isolated on a large, hollow foam polystyrene block, indicating the presence of significant parasitic capacitance from the test setup, particularly when the trap was measured with one terminal earthed.

Note : $Z_{eff} \approx (0.03 + 0.147f) + j(-6 + 23.3f)$ over the main frequency range of interest, f in MHz.

When re-tested on 14 Nov. braid losses had increased 24% relative to Sept. values, centre conductor losses by 15%.

⁴ Z_{eff} = impedance of the inductor L, and loss resistance R_{xp} , in parallel with winding stray capacitance, C_o

8. Impedance of Centre Conductor Inductor only at RF

Table 5 records the impedance of the inductor formed by the coaxial centre conductor only vs. frequency. Calculated $C_o = 5.3 \text{ pF}$ based on 6 – 12 MHz frequency doubling. Calculated Inductance $L = 4.15 \text{ } \mu\text{H}$

Using the "natural frequency" method at 40.06 MHz with auxiliary inductor of $0.2 \text{ } \mu\text{H}$

$C_o = 3.8 \text{ pF}$ $L = 4.17 \text{ } \mu\text{H}$ $R_{xp} = 84 \text{ k}\Omega$

Frequency	5.0	6.0	7.0	10.0	12.0	40.065
C_{dial}	238 pF	164 pF	119 pF	55 pF	37 pF	no change
$Q_{\text{indicated}}$	92	100	107	119	118	$\delta Q = -30$
$L_{\text{aux}} = 0.2 \mu\text{H}$: dial capacitance to resonate and Q with L_{aux} only : $\delta Q =$ change when test L added						66pF Q=220
Q_{true}	94	103	112	130	135	80
$Z_{\text{eff}} @ \text{freq.}$	$1.5 + j 134$	$1.6 + j 162$	$1.8 + j 191$	$2.4 + j 289$	$3.0 + j 359$	$84 \text{ k}\Omega + j 0$

Table 5 : Inductance of Inner Conductor only : measure between As and Af : all other leads open

9. Impedance of Short Circuited Coaxial Cable

Frequency	3.0	5.0	6.0	10.0	12.0	27.37
C_{dial}	4,900	1,760	1,226	415	275	no change
$Q_{\text{indicated}}$	15	20	22	26	27	53
$Z_{\text{eff}} @ \text{freq.}$	$0.7 + j 10.8$	$0.9 + j 18.1$	$1.0 + j 21.6$	$1.5 + j 38.3$	$1.8 + j 48$	$2.9 \text{ k}\Omega$
$L_{\text{aux}} = 0.2 \mu\text{H}$: dial capacitance to resonate and Q with L_{aux} only : $Q_{\text{ind}} =$ value when test L added						149pF Q=188

Table 6 : Inductance of Short Circuited Coax only : measure between As and Bs : short Af to Bf

Estimation of C_o by the frequency doubling method is meaningless as the current and voltage distribution changes dramatically with change of frequency. For the same reason, $C_o = 59.6 \text{ pF}$, calculated by the natural resonance method, is not the true effective capacitance at 27.37 MHz. For a quarter-wave shorted stub, for which the current measurement setup is a good approximation, the effective capacitance = $2/\pi$ times open circuit capacitance and effective inductance = $2/\pi$ times short circuit inductance. Z_{eff} for the $1/4 \lambda$ stub is meaningful.

Measured inductance $\approx 0.57 \text{ } \mu\text{H}$ including the inductance of the 55 mm long tails. The self-resonant frequency of 27.37 MHz is slightly below the frequency of a 1.67 m length of solid polyethylene dielectric coaxial cable due to the effect of the tails. True inductance between the centre and braid with the far end short circuited and the effects of connecting tail leads removed is probably about $3/4$ of the value measured, i.e. probably closer to $0.43 \text{ } \mu\text{H}$. This latter inductive value plus the resistive component of Z_{eff} is considered a better approximation to use if estimating the complex propagation coefficient for the coaxial cable, $\gamma = \alpha + j\beta$.

10. Capacitance of Coaxial Cable at RF

Effective capacitance and Q-factor of the coaxial cable at RF can be measured with the aid of an auxiliary inductor. At the test frequency L_{aux} is resonated with $C_{\text{dial}}@L_{\text{aux}}$ set to a larger value than the expected value of the cable capacitance and Q_{ind} is noted. Then the coaxial cable capacitance is connected in parallel with the Q-meter variable capacitance and resonance restored by adjusting C_{dial} . The new value of C_{dial} , designated $C_{\text{dial}}-C_{\text{cabl}}$, and new Q_{ind} , designated $Q_{\text{ind}} L_{\text{ux}}+C_{\text{cb}}$, are noted.

Normal connections to the cable are As and Bs, with Af and Bf normally open circuit, except where specially noted as "parallel" for 3MHz and 6MHz. At these two frequencies measurements were made both with the normal connection and also with As paralleled with Af and Bs paralleled with Bf, i.e. connections are made to both ends of the cable.

$$C_{cable} = C_{dial@L_{aux}} - C_{dial-C_{cabl}} \quad Q_{cap.cable} = \frac{Q_{indL_{aux}} \cdot Q_{indL_{ux}+C_{cb}}}{Q_{indL_{aux}} - Q_{indL_{ux}+C_{cb}}} \cdot \frac{C_{cable}}{C_{dial@L_{aux}} + C_{oa}}$$

C_{oa} = self capacitance of auxiliary inductor, L_{aux} . Note capacitor phase defect $\tan \delta X_C = 1/ Q_{cap.cable}$

Freq. MHz	L_{aux} μ H	C_{dial} @ L_{aux}	Q_{ind} for L_{aux}	$C_{dial} - C_{cable}$	Q_{ind} $L_{ux}+C_{cb}$	C_{cable}	$Q_{cap.cable}$
7.0	1.7	334	315	154	165	180 pF	190
6.0	1.7	456	295	280	208	176 pF	270
6 parallel	1.7	458	290	285	233	173 pF	415
4.8	4.6	225	220	51	150	174 pF	360
3.0	10 μ H	303	335	130	245	173 pF	490
3 parallel	10	301	340	130	263	171 pF	650
1.65	32	300	240	130	203	170 pF	730
0.906	100	300	350	130	295	170 pF	1,040
0.505	320 μ H	300	225	130	$\delta Q = -18.5$	170 pF	1,380
0.287	1000 μ H	301	330	132	$\delta Q = -32$	169 pF	1,640

Table 7 : Capacitance of Coaxial Cable : connect between As and Bs, except where " parallel " noted.

A clear trend is evident from Table 7 : as frequency is reduced the Q of the cable capacitance rises. At high frequencies the series reactive impedance of the capacitor is low while the series resistance of the conductors is now of significant magnitude relative to the magnitude of the capacitive reactance. So Q at high frequencies is dominated by the ratio of capacitive reactance $1/j\omega C$ to series conductor resistance R_s . At low frequencies $1/j\omega C$ is high relative to R_s , which is slowly decreasing due to reduced skin effect as frequency reduces. At low frequencies the dielectric loss becomes of increasing importance as a determinant of capacitor Q. For polyethylene dielectric this loss tends to be constant over the frequencies of interest so a reasonable assumption is for Q due to dielectric loss to approach 2,000, or $\tan \delta X_C \rightarrow 0.0005$. This value is considered appropriate when evaluating the $(j\omega C + G)$ term of γ , the cable complex propagation constant.

Rising effective capacitance with increasing frequency is also apparent : attributable to cancellation of the $-j$ reactance of the cable capacitance by the $+j$ reactance of the series inductance of the cable. Further evidence of this effect is provided by comparison of the 6.0 and 3.0 MHz results against the 6 (parallel) and 3 (parallel) results. By feeding signal to both ends of the cable simultaneously, series inductances are placed in parallel, reducing their effect on effective capacitance. Loss resistances of the conductors are also reduced by the parallel arrangement, leading to higher values of measured Q-factor.

11. VNA Measurements

Table 8 and Figure 3 have the impedance results from a coaxial VNA for the 'bootstrap' trap in the region of the fundamental, or lowest parallel resonance. Normalising resistance for the plot = 600 Ω. Whilst the resonance is evident, impedance values are too high to be measured accurately by an instrument intended for 50 Ω systems⁵ and frequencies in the VHF – UHF range.

MHz	3.5	4	5	5.5	6.1	6.4	6.7	7.0	8.0
Z _T Ω	7.5+j350	12+j470	44+j1k	120+j1k5	1k+j4k5	> 10k	2k-j6k3	330-j2k9	36-j1k1

Table 8 : VNA results for the Fundamental Parallel Resonance

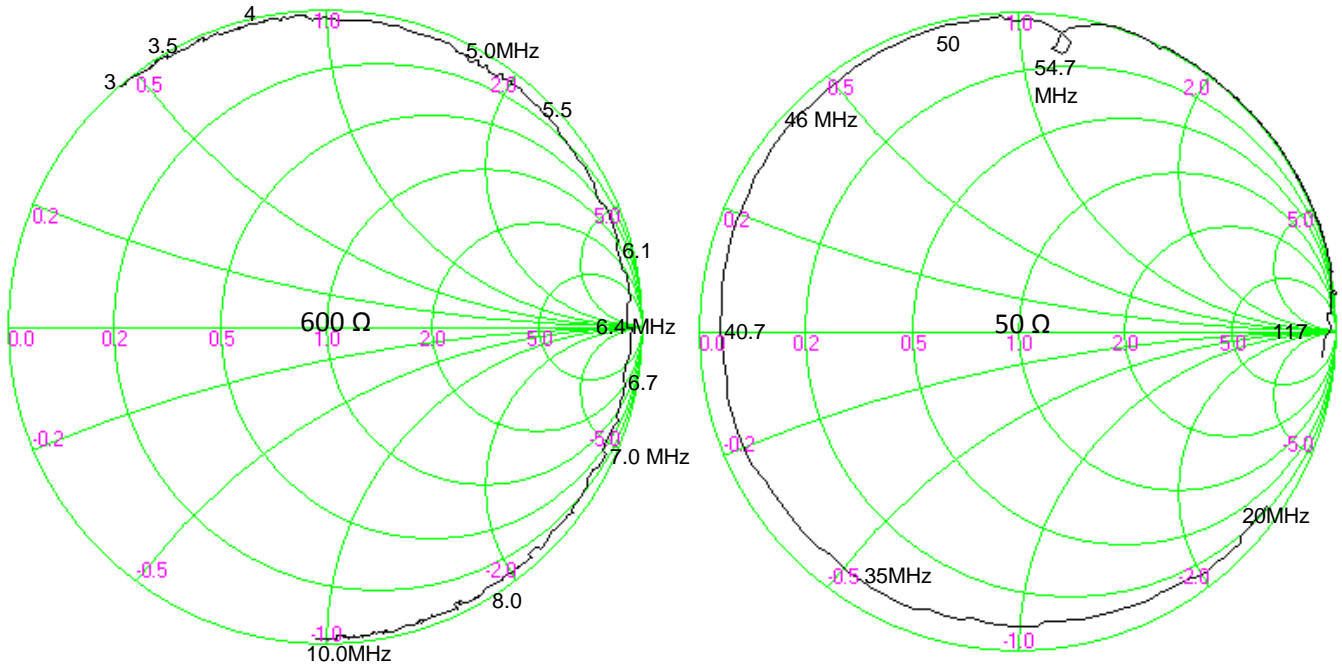


Fig. 3 : Fundamental Parallel Resonance (Z_n = 600 Ω) Fig. 4 : 1st Series + 2nd Parallel Resonance (Z_n = 50Ω)

Utility of the VNA is rapid identification of all resonances, both parallel and series, over a wide frequency range. Table 9 and Figure 4 have results for the lowest series resonance. Frequency of the series resonance was highly dependent on lead length. The second parallel resonance was in the region of 112 - 118 MHz, precise frequency varying noticeably in the presence of any adjacent objects.

MHz	35	40.6 (series resonance.)	45	50	54.7 (masked)	117 (// resonance)
Z _T Ω	2.5 – j 28	1.6 – j 0.6	1 + j 22	1 + j 40	7 + j 60	> 1k

Table 9 : VNA results for the Lowest Series Resonance

Two masked parasitic resonances were noted, at 54.7 MHz and approximately 60 MHz.. These resonances are internal, their full nature being not directly apparent at the measurement terminals due to other intervening network impedances. When fine grain results are plotted on a Smith Chart a masked resonance will often appear as a kink or as a small, localised, secondary loop on the impedance locus.

⁵ The VNA was modified for this test by substitution of a custom made directional coupler to interface to 600Ω systems.

12. Impedance Adjacent to Fundamental Resonance

f MHz	δf MHz	C_2	Q_a	δC_{+T}	Q_{+T}	Parallel $R_{xp} X_{xp}$	Series $r_{xseries} + X_{xs}$	Q_{ind}	Q_L	<i>Predicted</i>
4.00	-2.4	326	195	+69	118	36k j580	9.1 + j580	64	100	9.6+j600
5.00	-1.4	206	190	+28	117	47k j1.1k	27 + j 1.1k	41	105	29+j1k2
5.33	-1.0	180	185	+20	113	48k j 1.5k	46 + j 1.5k	33	100	52+j1k6
5.76	-0.6	154	185	+9.8	117	57k j 2.8k	140 + j 2.8k	20	110	142+j2k9
5.86	-0.5	149	185	+8.2	118	59k j 3.3k	180 + j 3.3k	18	112	205+j3k5
5.96	-0.4	143	182	+5.6	117	61k j 4.8k	370 + j 4.7k	13	114	315+j4k4
6.06	-0.3	139	183	+4.8	118	63k j 5.5k	470 + j 5.4k	11.5	116	560+j5k9
6.16	-0.2	134	180	+3.2	115	61k j 8.1k	1.0k + j 7.9k	7.9	110	1k2+j8k8
6.26	-0.1	130	177	+1.8	113	61k j 14k	3.1k + j 13k	4.2	108	4k8+j16k8
6.36	0	125	180	< 0.1	115	64k j ∞	64k + j 0	0	112	64k+j0
6.46	+0.1	121	175	- 0.9	113	65k -j 27k	9.8k - j 23k	2.3	112	4k8-j12k1
6.56	+0.2	117	175	-2.5	113	66k -j 9.7k	1.4k - j 9.5k	6.8	112	1k3-j9k1
6.66	+ 0.3	113	175	-3.8	112	66k -j 6.3k	590 - j 6.2k	10.5	110	570-j6k2
6.86	+0.5	107	170	- 5.4	110	68k -j 4.3k	270 - j 4.3k	16	110	210-j3k8
7.06	+ 0.7	100	170	- 7.6	110	71k - j 3.0k	126 - j 3.0k	24	112	107-j2k7
7.50		89	168	-14	101	60k - j 1.5k	38 - j 1.5k	39	89	50-j1k7
8.00		77	161	-17	95	59k - j 1.2k	23 - j 1.2k	52	82	28-j1k2

Table 10 : Measured Impedances Adjacent to the Fundamental Parallel Resonance

A variation on the auxiliary inductor method was used to measure the bootstrap trap impedance at frequencies close to the 6.3 MHz resonant frequency. Resonance was established with the auxiliary inductor alone at the frequency of interest, noting the Q and capacitance. Then the trap was placed in parallel with L_{aux} and resonance restored by adjusting the capacitance, noting the changes in Q and capacitance. Change in C_{dial} , = δC_{+T} , and knowledge of the frequency = ω permits calculation of trap parallel susceptance, while change in Q allows calculation of parallel conductance.

$$\text{Trap susceptance} = B_T = 1/X_T = - \delta C_{+T} \cdot \omega \quad (\text{and from eqn. of section 5}) \quad R_{xp} = \frac{Q_a \cdot Q_{+t}}{Q_a - Q_{+t}} \cdot \frac{1}{\omega_o \cdot C_2}$$

From the results given in Table 10, significant asymmetry is noticeable adjacent to the resonant frequency. This is considered to be attributable to difficulties in maintaining constant connecting lead dress, parasitic capacitances and parasitic losses as the Trap under test is repeatedly connected to, and disconnected from, the earthed test equipment and shielded. Other sources of error are the requirement to measure differences between large quantities that are comparable in magnitude, difficulty of precisely determining the trap resonant frequency, and the significant temperature coefficient of resonant frequency. Nevertheless comparison with results in Table 2 is reasonable for frequencies well removed from resonance. An error of 30 kHz in resonant frequency determination, or a discrepancy of 0.4 pF in lead capacitance can account for the asymmetry in the tabulated results

"Predicted" values are for a parallel resonant circuit with identical L-C ratio, having identical losses all concentrated in the inductor : a reasonably useful but not exclusive model⁶ for the Trap in the region of fundamental resonance.

⁶ see Zinn, M.K. "Network Representation of Transcendental Impedance Functions" BSTJ v.31, 1952, pp.378-404

Q_{ind} in the table is the indicated Q of the trap impedance at the tabulated frequency. It is simply the magnitude of parallel resistance divided by the parallel reactance. Q_L is the Q that the inductor alone would appear to possess if all of the losses were concentrated in the inductor. In reality a significant loss contribution is made by capacitive current flowing in the centre conductor of the coaxial cable, particularly above resonant frequency where overall reactance of the trap is capacitive. Hence the drop in Q_L observed at frequencies well above resonance.

$$Q_{ind} = R_{xp}/X_{xp} = X_{xseries}/I_{xseries} \quad Q_L = R_{xp}/\omega.14.3E-6 = Q_{ind}(1 + C_o/\delta C_{dial})$$

In the 2nd equation for Q_L include the sign for δC_{dial} , a negative Q value denotes that the trap is capacitive.

As a check on the measurement technique a 56 kΩ metal film resistor was measured using two different auxiliary inductors and 3 different Q-multiplier meter settings. Results were all in the range 56 – 62 kΩ shunted by 0.3pF.

13. Bridge Measurements of Impedance vs. Frequency

RF impedance bridges were used as a check on the results at frequencies away from resonance. A W-K model B801 was capable of very limited accuracy in the regions close to resonance as the smallest conductance dial calibration marks were at 0.05 mS intervals, corresponding to a 20k Ω parallel resistance. Estimates were made to 0.01mS. At regions away from resonance the limitation was a maximum susceptance equivalent to ± 200 pF at the measurement frequency. For the GR model 1606A the maximum equivalent series resistance was 1k Ω and maximum equivalent series reactance = ± 5k divided by frequency in MHz. Range extension at reduced accuracy was possible by use of an auxiliary capacitor.

A general rule for bridge accuracy should be noted : any minor component ≤ 1% of a major component magnitude is likely to have compromised accuracy, particularly if the major component is reactive.

MHz	2	2.5	3	3.5	4	5	6	6.06
B801			.03 -154p 4+ j345	.03 -102p 6+ j446	.03 -66p 11+ j603	.02 -27p 28+j1k2	.02 -3.7p 1k+j7k0	
1606A	3.2+ j205	4.1+ j276	5.8+ j360	8.5+ j480	13+j630	42+j1k5*	475+j5k3*	690+j6k3*
MHz	6.3	6.6	6.66	7	7.5	8	10	11
B801	.02 +0.2p 43k-j17k	.02 +4.4p 590-j5k4		.02 +9.2p 120-j2k5	.02 +14p 46-j1k5	.01 +18p 12-j1k1		.03 +34p 5.4-j425
1606A			570-j5k7*	164-j3k4*		23-j1k4*	5 – j740*	
MHz	12	15	20	25	30	40	42	45
B801		.03 +44p 1.7 - j241	.09 +58p 1.7 - j137	.21 +80p 1.3 - j80	.84 +134p 1.3 - j40	3.25 -186p 1.5 + j21		.71 -72p 1.7 + j49
1606A	2.4 - j370	1.6 - j246	1.2 - j153		1.1 - j65	1.2 - j7.5	1.4 + j1.3	

Table 11 : Measured Impedances using RF Bridges

Table 11 records the results for the two bridges. Raw dial readings have been tabulated for the B801, in the form of milliSiemens shunt conductance in parallel with picofarads shunt capacitance, together with the calculated impedance in order to illustrate the limited precision attainable. Comparison with earlier tabulated impedances reveals that generally the same trend is revealed by the bridge measurements, but accuracy is severely compromised, particularly for the minor component of impedance. Large differences between the B801 and 1606A in the region 30 – 45 MHz were caused by the different bridge zeroing techniques. For the 1606A the lead inductance of the trap could be calibrated out. For the B801 the lead inductance could not be calibrated out and no attempt has been made to subtract series reactance of the trap leads from the measured results.

Overall, RF bridges intended for antenna impedance measurements are not well suited to measuring trap impedances.

14. Impedance Magnitude Using Transmission Measuring Set

A transmission measuring set plus a test jig intended for characterising quartz crystals was used to measure the trap impedance magnitude and frequency at, and near resonance. Coaxial test leads of 0.5 m. length permitted the trap to be well isolated from earthed metal, supported on a hollow 8 cm. high foam polystyrene block. Measurements could be made rapidly at multiple frequencies without disturbing lead dress of the trap, thereby improving repeatability. Stray parasitic capacitance between the terminals of the test jig was ≈ 0.07 pF.

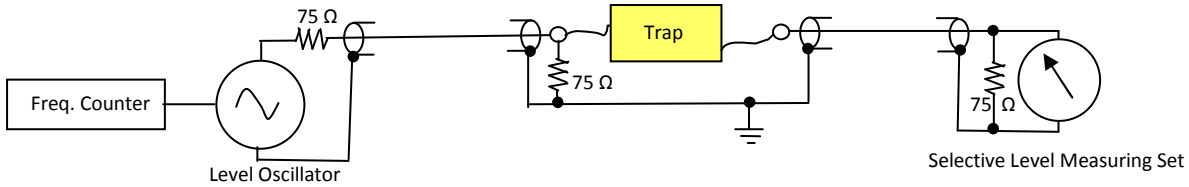


Fig. 5 : Transmission Measuring Set + Test Jig

MHz	5	6.087	6.187	6.287	6.387	6.487	6.587	6.687
Z Ω	1.1k	6.0 k	8.8 k	17.6 k	56.1 k	17.8 k	9.9 k	7.2 k

Table 12 : Impedance Magnitude vs. Frequency : Initial Test

Results on 20th October, recorded in Table 12, indicated $|Z| = 56.1$ kΩ at a resonance frequency of 6387 kHz at 21.0 °C ambient temperature. This was significantly lower than the measurements of section 12 taken in September, which were in turn lower than the measurements of Section 5 taken in August. Symmetry of measured impedance each side of resonance has improved due to the absence of handling that might otherwise disturb lead dress. General agreement with Table 10 is apparent. Since the test configuration was suitable for long term monitoring without disturbing lead dress it was decided to monitor changes with time and temperature.

The trap was exposed to noonday sun for 1 hour in a strong, dry NW breeze. A thermocouple junction was taped to the cylindrical former of the trap to measure its temperature. Trap temperature after exposure was 37.8 °C, resonant frequency 6424 kHz, impedance at resonance = 84.1 kΩ. Allowing the trap to slowly cool, resonant frequency 6408 kHz @ 28.5 °C, impedance 70.0 kΩ. Resonant frequency 6398.2 kHz @ 22.5 °C, impedance 59.6 kΩ.

On the following day the trap, supported on the foam polystyrene block, was placed inside a corrugated cardboard box with holes cut for the coaxial test leads and thermocouple. Two further large holes were cut, one as a vent and the other to allow prolonged injection of hot air from a hair dryer to create a hot, dry ambient for the trap.

Date	21 st Oct. Initial Heat Cycle				22 nd . Second Heat Cycle			23 rd . D (desiccant)			3 rd . (D)
Time H	0800	0845	1035	1230	0900	1205	1300	1030	1334	1545	1025
temp. °C	19.4°	48.4°	52.5°	53.5°	23.1°	53.1°	54.1°	22.5°	24.7	26.0°	18.3°
kHz	6389	6435	6442	6445	6387	6405	6406	6362	6369	6370	6358
Z Ω	62.4 k	89.1 k	91.2 k	91.2 k	58.2 k	84.1 k	84.2 k	54.3 k	55.6k	55.6 k	47.3k
Date	4 th Nov. cool to -20.2°, warm to amb., then heat cycle					5 th cool overnight to -16.9°, then slowly warm to room ambient					
Time H	1305	1320	1505	1512	1852	0946	0959	1018	1039	1144	1254
temp. °C	19.2°	39.3°	49.1°	40.0°	20.3°	-16.3°	-7.1°	+1.0°	+7.2°	+16.1°	+21.1°
kHz	6369	6384	6403	6398	6372	6376	6378	6382	6385	6390	6395
Z Ω	68.4 k	73.3k	82.2k	79.4k	60.3k	78.5k	74.1k	68.4k	66.1k	65.3k	66.1k

Table 13 : Impedance Magnitude During Heat Cycling

Table 13 summarizes results of multiple heating and cooling cycles and rest periods with desiccant over several days. After the 2nd. cycle the hot trap was sealed in a polythene bag along with freshly charged (blue) silica gel desiccant. This was then placed inside an airtight container and allowed to cool overnight before re-test as the room ambient changed during the course of the day. A further 10 days in desiccant ensued followed by re-test on 3rd. November. The trap was then cooled overnight to -20.2° C, allowed to warm rapidly⁷ to room ambient, then subjected to a 3rd. heat cycle on 4th. November. On the evening of 4th. the Trap, still attached to the test jig, was sealed into a polythene bag along with silica gel, then sealed into a small, thick walled foamed polystyrene box. Test leads for the jig and thermocouple were brought out of the box through a small hole. On testing the sealed assembly it was noted that the pressure exerted on the trap when squeezing it into the narrow confines of the box had raised the resonant frequency by 23 kHz and improved the parallel loss resistance to 73.3k. The whole assembly was then subjected overnight to a temperature of -16.9° C. On 5th. the cold trap was measured as it slowly warmed to room ambient. Only selected representative results are presented in Table 13 for the sake of brevity and to demonstrate trends. During the heating and cooling cycles results were generally noted for every 3° change of temperature, objective being to look for any sudden changes that might indicate a phase change for moisture or other compounds present : none were observed.

At the conclusion of each cycle a period of 1 hour was generally allowed for temperature to become uniform throughout the bulk of the trap, waiting for the strains caused by thermal gradients to subside. Evidence for thermal gradients can be seen in the results for 1320 vs. 1512 for 4th.November. For cooling cycles it is to be noted that a phase change for the tin plating of the conductors would have been initiated by the cold temperatures. Above +18° C white tin is the stable crystalline structure : below this temperature tin metamorphoses to grey tin, a brittle and more voluminous form. Speed of change depends on the temperature.

Interim conclusion is that the trap shows significant variations of frequency and impedance with handling, changes of ambient temperature, temperature cycles and time. Severe temperature cycling is possibly accelerating normal ageing effects by relief of stresses and resultant strains that occurred during fabrication.

Temperature Coefficients

Measurement of the temperature coefficient of inductance for the bootstrapped Trap was carried out at $\omega = 10,000$ radians/sec. for both hot and cold cycles, with time to stabilize at the temperature extremes to minimize temperature gradients. Resultant was confounded by the ageing effects of temperature cycling and by thermal gradients at intermediate stages during the cycling, but was considered to be $\leq +4 \text{ E-5}$ parts per ° C once temperature had been allowed to stabilize. With temperature gradients present, transient changes of inductance $\approx 1 \text{ E-3}$ parts / °C could be observed, persisting over periods of 10 minutes.

Temperature coefficient of series resistance = + 0.0039 / °C over the range -15°C to +50°C, the temperature coefficient of resistance for copper. Inductance and resistance values are given in Table 14. These are slightly higher than those in Table 1 due to the additional lead lengths necessitated by the presence of the polystyrene enclosure.

Temp °C	-14.5	-10.0	-8.6	-6.0	-2.0	0.0	+3.0	+6.0	+13.4	+23.0	+26.0
Time H	0935	0939	0940	0944	0951	0955	1002	1011	1050	1155	1257
L μH	14.98	14.92	14.90	14.96	14.97	14.96	14.97	14.96	14.96	15.00	15.00
r milli Ω	109.6	110.6	111.1	118.0	115.2	116.7	118.4	125.2	125.2	130.1	132.6

Table 14 : Inductance and Series Resistance vs. Temperature for Cold Cycle

Temperature coefficient of capacitance for the coaxial cable $\approx -3 \text{ E-4}$ parts / °C, a value that remained predictable and reversible over the range -15°C to +56°C. When time is allowed for temperature gradients to subside, the temperature

⁷ A layer of moisture condensed on the cold surface during warming to room ambient. Measurement during this cycle suggested that the layer of moisture had little effect on trap impedance.

coefficient of capacitance is an order of magnitude greater than the coefficient for inductance. With large temperature gradients present in the trap the situation can reverse.

Conclusions

1. Impedance at resonance is highest for the bootstrap trap configuration. Half-trap configurations present impedances $\approx \frac{1}{4}$ of the impedance for the bootstrap configuration.
2. Effective inductance for the bootstrap trap can be initially estimated :
 $\approx 2 \times \text{braid } L + 2 \times \text{mutual } L \text{ braid-to-centre-conductor} + \text{coax } L \text{ with far end looped}$
 $\approx 4 \times \text{braid inductance} + \text{coax inductance with far end looped.}$
Plus a small additional inductance for the lead connection A_f to B_s (see Fig. 1)
3. Effective capacitance for the bootstrap trap can be estimated :
 $\approx 0.25 \times \text{Coaxial Cable Capacitance} + 0.25 \times \text{stray inter-turn capacitance of braid winding.}$
This follows directly as both capacitances are connected across halves of the autotransformer formed by the series aiding connection of the centre conductor winding and the braid winding.
4. Effective Q-factor for the trap tends to peak at the resonant frequency. Below resonance Q decreases as the reactance of the inductance decreases faster than the effective series resistance. Above resonance the Q decreases because the increasing series resistance of the coaxial centre conductor dominates the losses in the capacitor.
5. Ageing effects on the resonant frequency are present. These could be critical if the trap function is to simply isolate a section of an antenna at the trap parallel resonant frequency. They are less likely to be critical if the trap is intended to add series inductance below its resonance in order to electrically lengthen an antenna to bring the antenna to resonance, and to add series capacitance above trap resonance in order to electrically shorten the same antenna and bring it to a second resonance.
6. Changes of resonant frequency with temperature are present. Criticality is as for ageing effects. For slow temperature changes the temperature coefficient of capacitance predominates. If significant temperature gradients are present then inductance fluctuations can be significant.
7. Stresses caused by temperature fluctuations or physical handling have a tendency to temporarily reduce trap losses, raising impedance at resonance. Effects subside with the passage of time. Possible cause is reduction of contact resistance between individual wire strands, particularly in the shield braid.
8. For highly critical applications, ageing prior to deployment is advisable. Temperature cycling for accelerated ageing is one potential treatment to reduce stress-strain effects.
9. Since the trap coaxial ends had not been sealed, effects of possible weatherproofing were not studied.
10. Secondary resonances are well separated from the primary parallel resonance. These secondary resonances are unlikely to have any practical utility for trap deployment.

Recommendations

1. Use the results presented above as a guide in design of resonant traps.
2. Other possible trap configurations could be studied such as, use of 75Ω cable, effects of spacing turns vs. close winding, use of Teflon cable such as RG142 with TFE Teflon dielectric and FEP Teflon sheathing.
3. Study the effects of different weatherproofing, sealing and UV protection treatments.
4. Allow ageing prior to deployment of traps in narrowband configurations where tuning is critical.

Ross Beaumont
VK2KRB

ver.2 : 20Nov'11 : note added in Section 7